Article

Alloyed Heterostructures of CdSe$_x$S$_{1−x}$ Nanoplatelets with Highly Tunable Optical Gain Performance

Yusuf Kelestemur,[†,§] Didem Dede,[†,§] Kivanc Gungor,[†] Can Firat Usanmaz,[†] Onur Erdem,[†] and Hilmi Volkan Demir*,[†,‡]

[†]Department of Electrical and Electronics Engineering, Department of Physics, UNAM−Institute of Materials Science and Nanotechnology, Bilkent University, Ankara 06800, Turkey

[‡]Luminous! Center of Excellence for Semiconductor Lighting and Displays, School of Electrical and Electronic Engineering, School of Physical and Materials Sciences, School of Materials Science and Nanotechnology, Nanyang Technological University, Singapore 639798, Singapore

Ⓢ *Supporting Information*

ABSTRACT: Here, we designed and synthesized alloyed heterostructures of CdSe$_x$S$_{1−x}$ nanoplatelets (NPLs) using CdS coating in the lateral and vertical directions for the achievement of highly tunable optical gain performance. By using homogeneously alloyed CdSe$_x$S$_{1−x}$ core NPLs as a seed, we prepared CdSe$_x$S$_{1−x}$/CdS core/crown NPLs, where CdS crown region is extended only in the lateral direction. With the sidewall passivation around inner CdSe$_x$S$_{1−x}$ cores, we achieved enhanced photoluminescence quantum yield (PL-QY) (reaching 60%), together with increased absorption cross-section and improved stability without changing the emission spectrum of CdSe$_x$S$_{1−x}$ alloyed core NPLs. In addition, we further extended the spectral tunability of these solution-processed NPLs with the synthesis of CdSe$_x$S$_{1−x}$/CdS core/shell NPLs. Depending on the sulfur composition of the CdSe$_x$S$_{1−x}$ core and thickness of the CdS shell, CdSe$_x$S$_{1−x}$/CdS core/shell NPLs possessed highly tunable emission characteristics within the spectral range of 560−650 nm. Finally, we studied the optical gain performances of different heterostructures of CdSe$_x$S$_{1−x}$ alloyed NPLs offering great advantages, including reduced reabsorption and spectrally tunable optical gain range. Despite their decreased PL-QY and reduced absorption cross-section upon increasing the sulfur composition, CdSe$_x$S$_{1−x}$ based NPLs exhibit highly tunable amplified spontaneous emission performance together with low gain thresholds down to ∼53 μJ/cm^2.
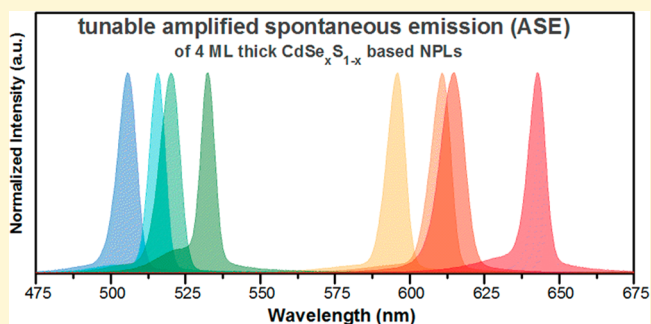
INTRODUCTION

Atomically flat semiconductor nanoplatelets (NPLs), also known as colloidal quantum wells, are an astonishing class of solution-processed semiconductor nanocrystals for the next-generation optoelectronic devices.[1,2] These NPLs with well-defined vertical thicknesses show distinguishable features compared to their counterparts.[3] They exhibit narrow emission bandwidth (∼40 meV),[4] giant oscillator strength with ultrafast fluorescence lifetime,[4] extremely large linear and nonlinear absorption cross sections,[5] and suppressed Auger recombination (AR).[6] In addition to these, their higher gain coefficient, broader gain bandwidth, and longer gain lifetime make them highly desirable for practical lasing applications.[7] In this respect, optical gain and lasing performances of core-only,[7−12] core/crown,[11] core/shell,[7,9,10,13] and core/crown/shell[10] NPLs have been studied extensively. Although core-only NPLs generally exhibit relatively higher gain threshold with low photostability, the synthesis of different heterostructures further reduces their gain thresholds to record low levels with enhanced photostability. However, due to the pure vertical quantum confinement observed in NPLs, their optical gain and lasing

performances are limited in terms of spectral tunability compared to colloidal quantum dots (CQDs). For example, 4 monolayer (ML) thick CdS and CdSe core NPLs exhibit discrete amplified spontaneous emission (ASE) peaks at ∼432[9] and ∼534 nm,[12] respectively.

To obtain tunable excitonic properties in a wide spectral range, colloidal synthesis of NPLs with different vertical thicknesses, heterostructures, and compositions have been studied. By optimizing the synthesis conditions, core-only NPLs having different thicknesses can be synthesized to tune their optical properties.[14] However, owing to pure vertical confinement observed in NPLs, they exhibit discrete emission and absorption behavior regardless of their lateral size. For example, CdSe NPLs having 3, 4, and 5 ML of vertical thicknesses terminated by Cd atoms on both sides always exhibit emission peak at ∼460, 513, and 550 nm, respectively.[14] In addition, core/crown[15−19] and core/shell[20,21] heterostruc-

tures of NPLs have been synthesized to further extend their spectral tunability. Nonetheless, the resulting excitonic properties of core/crown and core/shell NPLs have been shown to be strongly dependent on the vertical thickness of the starting core NPLs. For instance, 4 ML thick CdSe/CdS and CdSe/CdTe core/crown NPLs always exhibit similar emission behavior independent of their crown size. In addition to the colloidal synthesis of NPLs with different heterostructures, CdTe[22] and CdS[23] based NPLs have been synthesized to obtain tunable excitonic properties. Even though a pure population of CdS and CdTe NPLs having different vertical thicknesses have been synthesized successfully, they suffer from the lower photoluminescence quantum yield (PL-QY) and stability issues.

To achieve further tunable excitonic properties in colloidal NPLs, homogeneous alloying can be used as a highly effective approach, which has not been studied extensively. Previously, several studies have reported the synthesis of homogeneously alloyed $CdSe_xS_{1-x}$ core-only NPLs, showing tunable absorption spectra by adjusting the sulfur compositions.[24,25] However, the synthesized $CdSe_xS_{1-x}$ core-only NPLs exhibit low PL-QY ($\sim$10−20%) with the limited emission tunability in the spectral range of $\sim$490−510 nm.[26] Therefore, engineered heterostructures of alloyed NPLs have been greatly required to obtain enhanced excitonic properties, enabling the achievement of highly tunable and low-threshold gain performance.

To overcome these limitations, we synthesized core/crown and core/shell heterostructures of $CdSe_xS_{1-x}$ alloyed core NPLs and systematically studied their resulting excitonic properties, including spontaneous emission and stimulated emission performance. By synthesizing $CdSe_xS_{1-x}$/CdS core/crown NPLs, we achieved enhanced PL-QY (up to 60%), without changing the emission spectrum of $CdSe_xS_{1-x}$ alloyed core NPLs. Furthermore, with the synthesis of $CdSe_xS_{1-x}$/CdS core/shell NPLs, we further extended the tunable emission behavior of $CdSe_xS_{1-x}$ NPLs. These effective excitonic properties of alloyed core/crown and alloyed core/shell heterostructures with the reduced reabsorption enabled us to achieve highly tunable optical gain performance from $CdSe_xS_{1-x}$ based NPLs. Compared to CdSe core based NPLs, these $CdSe_xS_{1-x}$ based NPLs with relatively low gain thresholds are highly promising candidates for future lasing applications.

■ EXPERIMENTAL SECTION

Chemicals. Cadmium nitrate tetrahydrate $[Cd(NO_3)_2 \cdot 4H_2O]$ (99.999% trace metals basis), cadmium acetate dihydrate [Cd-$(OAc)_2 \cdot 2H_2O]$ (>98%), sodium myristate (>99%), technical-grade 1-octadecene (ODE), selenium (Se) (99.999% trace metals basis), sulfur (S) (99.998% trace metals basis), technical-grade oleic acid (OA) (90%), technical-grade oleylamine (OAm) (70%), N-methylformamide (NMF) (99%), and ammonium sulfide solution (40−48 wt % in H_2O) were purchased from Sigma-Aldrich. Hexane, ethanol, methanol, toluene, and acetonitrile were purchased from Merck Millipore and used without any further purification.

Preparation of Cadmium Myristate. For the preparation of cadmium myristate, we followed a previously published recipe in the literature.[15] In a typical synthesis, 1.23 g of cadmium nitrate tetrahydrate was dissolved in 40 mL of methanol and 3.13 g of sodium myristate was dissolved in 250 mL of methanol by continuous stirring. When the complete dissolution was achieved, both solutions were mixed and stirred around 1 h. Then, bulky solutions of cadmium myristate were centrifuged and precipitates dissolved in methanol for further cleaning. For the complete removal of excess precursors and better purification, this procedure was repeated at least three times. At the end, the precipitated part was dried under vacuum overnight.

Synthesis of the 4 ML thick $CdSe_xS_{1-x}$ Alloyed Core NPLs. For the synthesis of 4 ML thick $CdSe_xS_{1-x}$ alloyed core NPLs, we modified the commonly used recipe of 4 ML thick CdSe core NPLs.[15] 340 mg of cadmium myristate, 20 mg Se, and 30 mL of ODE were added in a 100 mL three-neck flask. The solution was degassed under vacuum at 95 °C around 1 h. Then, the temperature of the solution was set to 240 °C under argon flow. At 100 °C, the desired amount of sulfur precursor (S/ODE, 0.2 M) was injected rapidly to tune the composition of $CdSe_xS_{1-x}$ alloyed core NPLs. For example, for the synthesis of $CdSe_xS_{1-x}$ NPLs having sulfur composition $(1 - x)$ of 0.15, 0.25 and 0.30, we injected 0.25, 0.50, and 1.00 mL of sulfur precursors, respectively. When the temperature reached $\sim$195 °C, 70 mg of cadmium acetate dihydrate was added. After 10 min growth at 240 °C, 1 mL of OA was injected and the solution was moderately cooled to room temperature. Below 120 °C, 5 mL of hexane was injected for better dissolution of NPLs. In the purification state, NPLs were precipitated by addition of ethanol and then kept in hexane solution.

Thanks to the formation of alloyed $CdSe_xS_{1-x}$ NPLs, the resulting optical properties can be determined with the injected amount of S precursor. Moreover, the temperature at which cadmium acetate dihydrate is added is important to eliminate the formation of other species having different emission properties.

Preparation of Anisotropic Growth Solution for CdS Crown Region. For the lateral growth of CdS crown region, Cd and S precursors were prepared according to the well-known procedure with slight modifications.[15] 480 mg of Cadmium acetate dihydrate, 340 μL of OA, and 2 mL of ODE were loaded in a 50 mL three-neck flask. The solution was heated to 120 °C under ambient atmosphere with rigorous stirring and was also regularly sonicated. Alternating steps of heating and sonication followed until whitish homogeneous gel formed. When the cadmium precursor was ready, it was mixed with a 3 mL of S/ODE (0.1 M) precursor and then used for the coating of CdS crown for the alloyed NPLs.

Synthesis of 4 ML-Thick $CdSe_xS_{1-x}$/CdS Core/Crown NPLs. For the lateral growth of alloyed $CdSe_xS_{1-x}$ cores with CdS crown region, 5 mL of ODE, 100 μL of OA, and 1 mL of 4 ML-thick $CdSe_xS_{1-x}$ dissolved in hexane (100 μL $CdSe_xS_{1-x}$ NPLs dissolved in 3 mL of hexane having an optical density of $\sim$1 at 350 nm) were loaded into a 50 mL three-neck flask and degassed at 80 °C for the removal of excess solvents. Under an argon flow, the solution was heated up to 240 °C. Around 190−195 °C, the injection of CdS anisotropic growth mixture was started and 0.70 mL of this mixture was injected at a rate of 8 mL/h. The amount of injected precursor determines the crown size with the desired optical properties. After the injection of the anisotropic growth mixture, $CdSe_xS_{1-x}$/CdS core/crown NPLs were further annealed at 240 °C for 5 min and cooled down to room temperature. For the cleaning of the resulting core/crown NPLs, ethanol was used for precipitation and then the precipitated NPLs were dissolved in hexane.

Synthesis of $CdSe_xS_{1-x}$/CdS Core/Shell NPLs. By using the colloidal atomic layer deposition (c-ALD) technique, $CdSe_xS_{1-x}$/CdS core/shell NPLs were synthesized.[21] In accordance with this well-known procedure, 3 mL of N-methylformamide (NMF) and 3 mL of core NPLs dissolved in hexane were mixed. With the addition of 50 μL of sulfur precursor [ammonium sulfide solution (40−48 wt % in H_2O)], NPLs were transferred from nonpolar hexane to highly polar NMF. For a complete sulfur coating, the solution was stirred around 5 min and excess sulfur was removed in the following washing steps. In this step, acetonitrile and toluene were added to precipitate NPLs and then 3 mL of fresh NMF was added for complete dissolution. For the next cadmium deposition step, 2 mL of cadmium precursor (0.2 M cadmium acetate dihydrate in NMF) was added and and waited for 5 min for the reaction. The NPLs were then precipitated with the addition of acetonitrile and toluene. As a result of these processes, 1 ML CdS shell was formed on the $CdSe_xS_{1-x}$ alloyed core NPLs. To increase the shell thickness, this process was repeated in a similar way. Finally, with the addition of OAm to the solution of NPLs terminated by Cd atoms, core/shell NPLs dissolved in NMF can be transferred to hexane.
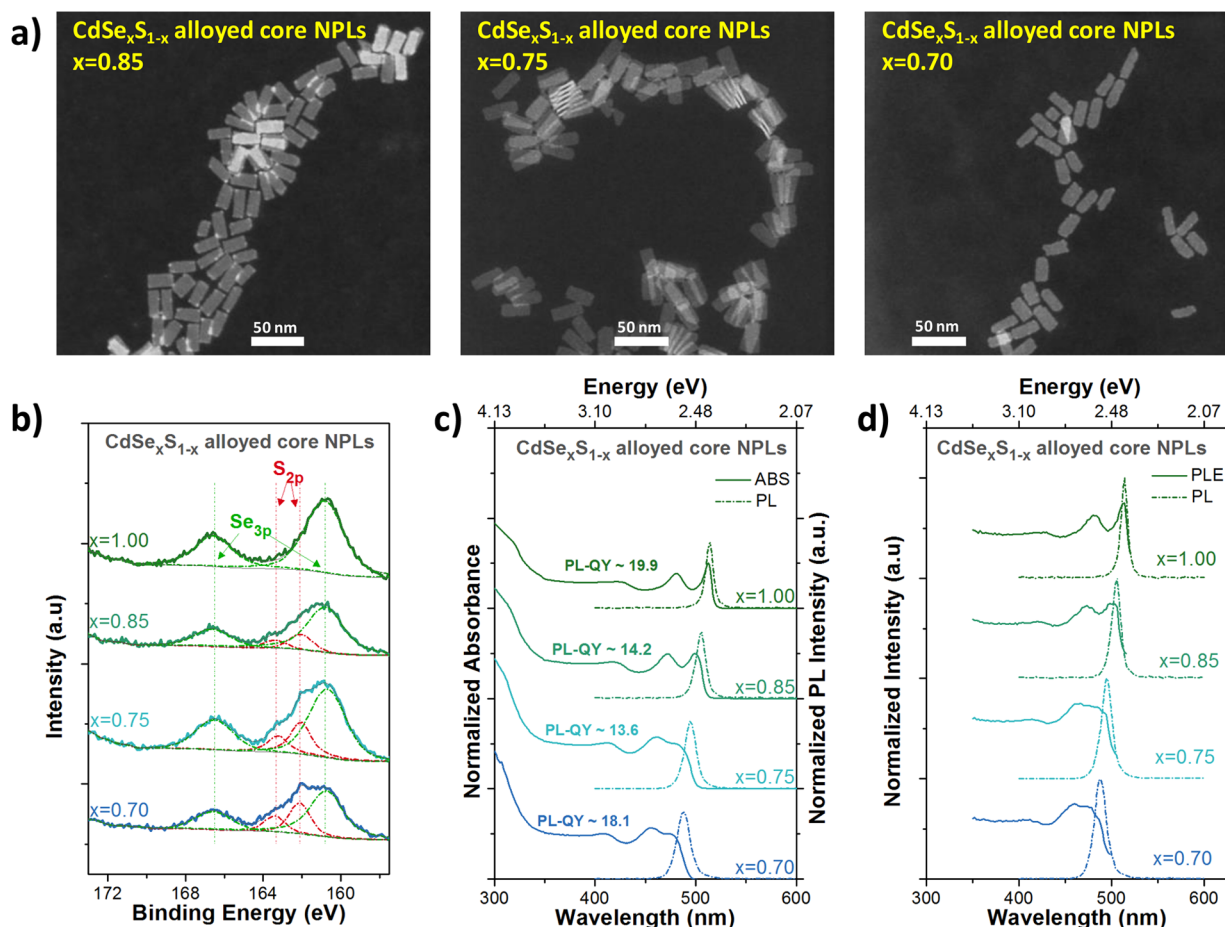
Figure 1. (a) HAADF-STEM images of CdSe$_x$S$_{1-x}$ alloyed core NPLs having different sulfur compositions, (b) high-resolution X-ray photoelectron spectra of spin-coated thin films of CdSe$_x$S$_{1-x}$ alloyed core NPLs, (c) absorbance and photoluminescence (PL) spectra of CdSe$_x$S$_{1-x}$ alloyed core NPLs, showing continuous blue-shifted excitonic features, and (d) photoluminescence excitation (PLE) spectra of CdSe$_x$S$_{1-x}$ alloyed core NPLs.

Absorption and Steady-State Photoluminescence. UV−vis absorption and photoluminescence spectra of NPLs together with their photoluminescence excitation spectra were taken by using Cary 100 UV−vis and Cary Eclipse fluorescence spectrophotometer, respectively.

Photoluminescence Quantum Yield (PL-QY) Measurements. The PL-QY measurements of NPLs were performed according to the methodology described by de Mello et al.[27] Our PL-QY measurement setup was equipped with an Ocean Optics Maya 2000 spectrometer, an integrating sphere, a xenon lamp and a monochromator. For the PL-QY measurements, freshly prepared dispersion samples of core only, core/crown and core/shell NPLs were used and excited at a wavelength of 400 nm.

Time-Resolved Photoluminescence Spectroscopy. The time-resolved photoluminescence measurements were taken by using Pico Quant FluoTime 200 spectrometer. Dispersion samples of NPLs were excited with a picosecond pulsed laser having a wavelength of 375 nm, and the fluorescence decay curves were recorded with TimeHarp time-correlated single-photon counting (TCSPC) unit. The FluoFit software was used for the reconvolution mode fitting of the decay curves to account for the instrument response function (IRF).

Transmission Electron Microscopy (TEM). TEM images of NPLs were acquired with FEI Tecnai G2 F30 operated at 300 kV in the high-angle annular dark-field scanning transmission electron microscopy (HAADF-STEM) configuration. For the sample preparation, NPLs were cleaned with ethanol at least two times to remove excess ligands. Then, 5 μL of diluted NPL solution was dropped on a 200 mesh copper grid and kept under vacuum for the complete drying before the imaging.

X-ray Photoelectron Spectroscopy (XPS). To determine the elemental composition of alloyed CdSe$_x$S$_{1-x}$ core NPLs, we performed XPS measurements by using the Thermo Scientific K-Alpha X-ray photoelectron spectrometer. The samples for XPS were prepared by spin-coating of NPL solutions on the silicon substrates (∼1 × 1 cm^2). The acquired high-resolution spectra of CdSe$_x$S$_{1-x}$ core NPLs with varying sulfur compositions were analyzed by using the Avantage software.

■ **RESULTS AND DISCUSSION**

In this study, we prepared CdSe$_x$S$_{1-x}$ alloyed NPLs together with their core/crown and core/shell heterostructures to obtain highly tunable excitonic properties. First, we started with the synthesis of 4 ML thick CdSe$_x$S$_{1-x}$ core NPLs having an additional layer of Cd atoms and used them as a seed for the further synthesis of core/crown and core/shell NPLs. For the synthesis of CdSe$_x$S$_{1-x}$ core NPLs, we modified the recipe of 4 ML thick CdSe core NPLs (see the experimental section for details).[15] By the addition of a certain amount of sulfur precursor after degassing, we succeeded in the formation of a highly uniform CdSe$_x$S$_{1-x}$ alloy, and depending on the amount of injected sulfur precursor, the composition of CdSe$_x$S$_{1-x}$ was tuned in a precisely controlled way. The high-angle dark-field scanning transmission electron microscopy (HAADF-STEM) images of CdSe$_x$S$_{1-x}$ alloyed core NPLs with various compositions feature a rectangular shape and uniform size distribution regardless of the sulfur composition (Figure 1a). While lateral sizes of CdSe$_x$S$_{1-x}$ alloyed core NPLs
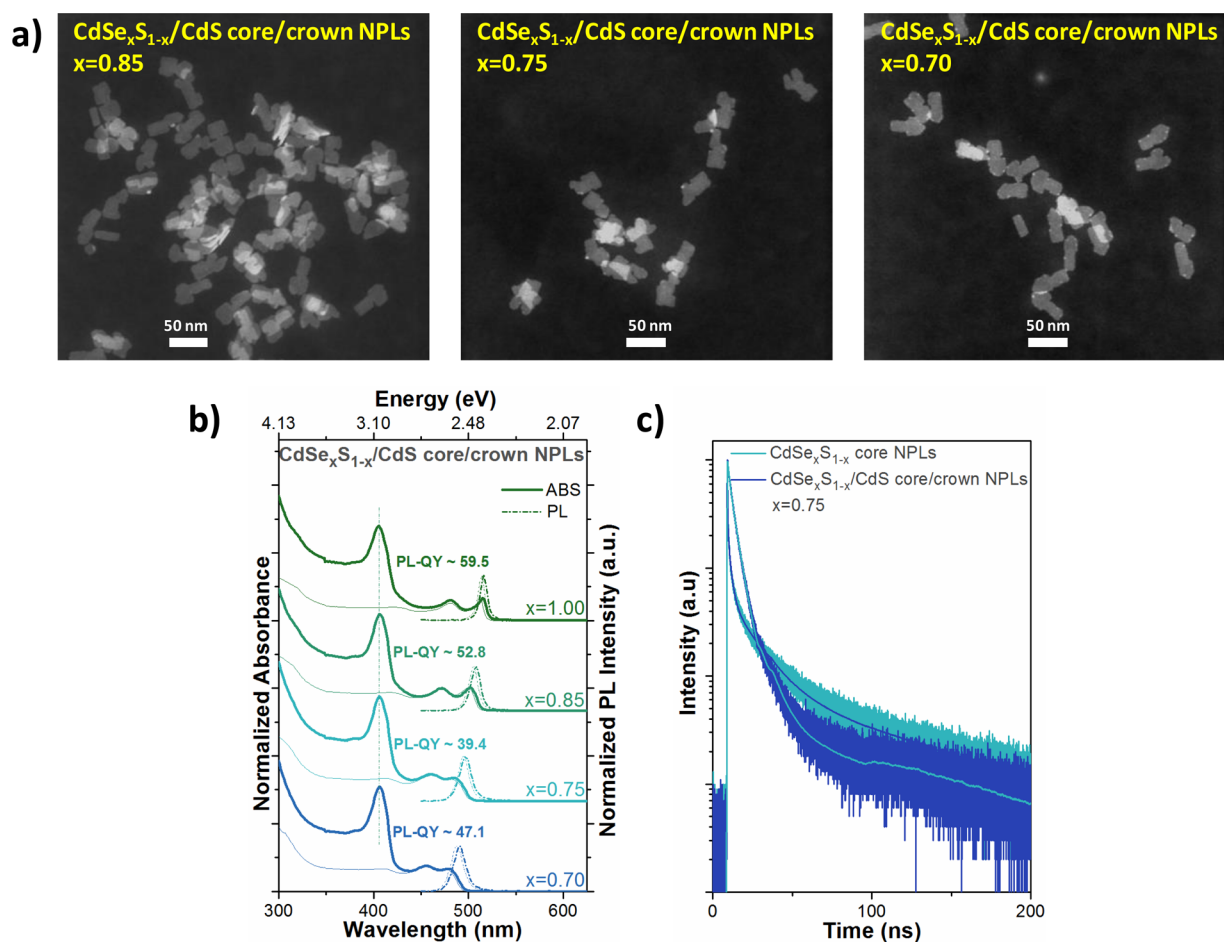
Figure 2. (a) HAADF-STEM images of CdSe$_x$S$_{1−x}$/CdS alloyed core/crown NPLs having different sulfur compositions, (b) absorbance and photoluminescence spectra of CdSe$_x$S$_{1−x}$/CdS core/crown NPLs, and (c) time-resolved fluorescence decay curves of CdSe$_x$S$_{1−x}$ alloyed core and CdSe$_x$S$_{1−x}$/CdS core/crown NPLs for the case of x = 0.75.

were observed to be generally increased with increasing the amount of sulfur, their thicknesses were found to be the same with the 4 ML thick CdSe core only NPLs. Also, the elemental composition of CdSe$_x$S$_{1−x}$ alloyed core NPLs is determined by using X-ray photoelectron spectroscopy (XPS) (Figure 1b). It was measured that the elemental composition of sulfur can be increased up to (1 − x) = 0.30 with a 1 mL of sulfur precursor injection. Further increasing the amount of sulfur resulted in the formation of a mixed population of NPLs with excess amounts of colloidal quantum dots so that it is not easy to achieve pure population of CdSe$_x$S$_{1−x}$ alloyed core NPLs with cleaning procedures.

After structural characterization of CdSe$_x$S$_{1−x}$ alloyed core NPLs having the same vertical thicknesses, we performed optical characterization including absorption, photoluminescence (PL), and photoluminescence excitation (PLE) spectroscopy. Absorption spectra of CdSe$_x$S$_{1−x}$ alloyed core NPLs are presented in Figure 1c. From the absorption spectrum of CdSe core NPLs, splitting of sharp excitonic features including light-hole (~480 nm) and heavy-hole (~512 nm) transitions are clearly visible, indicating formation of the quantum well like electronic structure.[4] In CdSe$_x$S$_{1−x}$ alloyed core NPLs, these sharp excitonic features were slightly broadened and continuously shifted to higher energies by increasing the sulfur composition. Also, the PL of CdSe$_x$S$_{1−x}$ alloyed core NPLs exhibits similar behavior with the absorption. For example,

while the CdSe core only NPLs have their emission peak at ~513 nm with a full-width-at-half-maximum (fwhm) of ~40 meV, the CdSe$_x$S$_{1−x}$ alloyed core NPLs having the highest sulfur composition of (1 − x) = 0.30 possess theirs at ~488 nm with a fwhm of ~80 meV. Here the blue-shifting in excitonic features can be explained with the increase of the energy band gap due to the alloying. On the other hand, slight broadening could be attributed to the variation in the composition and/or inhomogeneous alloying of NPLs. However, the similar excitonic transitions observed from the PLE spectra of CdSe$_x$S$_{1−x}$ core NPLs taken at different emission wavelengths has ruled out this possibility and strongly suggested the formation of CdSe$_x$S$_{1−x}$ core NPLs having a homogeneously alloyed crystal structure (Figure S3). Therefore, the broadening of the excitonic features may most likely be due to the enhanced exciton−phonon coupling commonly observed in this material system.[28]

Although the emission of the CdSe$_x$S$_{1−x}$ alloyed core NPLs was demonstrated to be shifted to higher energies with increasing sulfur composition, they suffered from the decreased PL-QY (~10−20%) and the stability issue with respect to the CdSe core only NPLs, which can be explained with the increased surface trap sites owing to their extended lateral size (Figure S1). To achieve better optical properties and enhanced stability without changing the emission behavior of CdSe$_x$S$_{1−x}$ alloyed core NPLs, we synthesized CdSe$_x$S$_{1−x}$/CdS core/crown
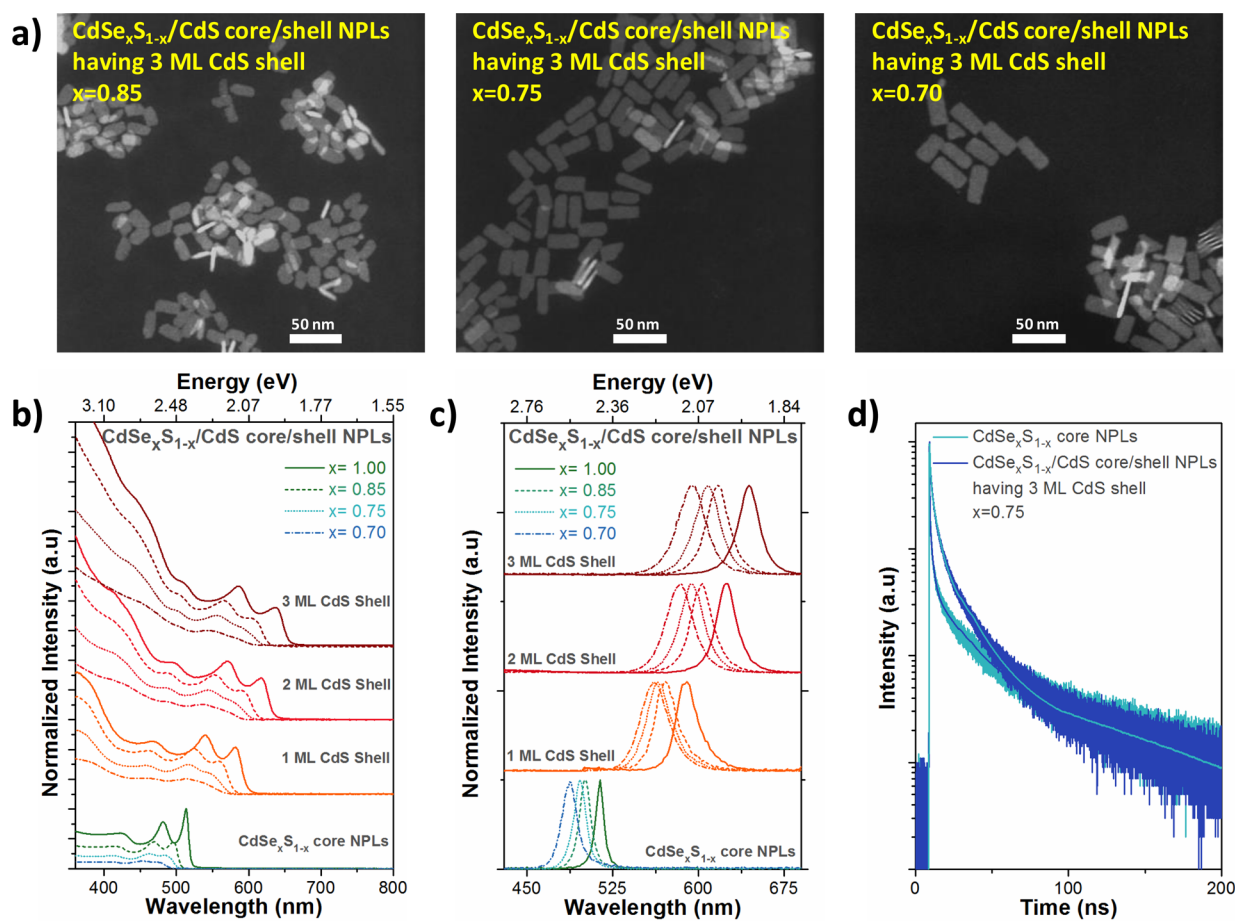
Figure 3. (a) HAADF-STEM images of CdSe$_x$S$_{1-x}$/CdS core/shell NPLs having 3 ML CdS shell thicknesses, (b) absorbance spectra of CdSe$_x$S$_{1-x}$/CdS core/shell NPLs with different sulfur composition and CdS shell thicknesses, (c) PL spectra of CdSe$_x$S$_{1-x}$/CdS core/shell NPLs with varying sulfur composition and CdS shell thicknesses, and (d) time-resolved fluorescence decay curves of CdSe$_x$S$_{1-x}$ alloyed core and CdSe$_x$S$_{1-x}$/CdS core/shell NPLs having 3 ML CdS shell for the case of $x = 0.75$.

NPLs. The formation of CdS crown extension only in the lateral direction and passivation of sidewalls can greatly enhance the PL-QY of NPLs without changing the spectral position of the emission.[10] By using the freshly synthesized CdSe$_x$S$_{1-x}$ alloyed core NPLs as seeds, we prepared core/crown NPLs using a slightly modified recipe (see the experimental section for details). HAADF-STEM images of CdSe$_x$S$_{1-x}$/CdS core/crown NPLs having different sulfur compositions are shown in Figure 2a. In comparison to CdSe$_x$S$_{1-x}$ core NPLs, lateral sizes of the core/crown NPLs are found to be increased, while the vertical thicknesses remained the same, suggesting the formation of core/crown heterostructures. It is also important to note that, although we used highly uniform and rectangular-shaped CdSe$_x$S$_{1-x}$ alloyed core NPLs as seeds, the formation of the CdS crown region was nonuniform in the lateral direction, which is typically observed for the CdSe/CdS core/crown NPLs in literature.[11,15,16]

Compared to the CdSe$_x$S$_{1-x}$ core NPLs, CdSe$_x$S$_{1-x}$/CdS core/crown NPLs exhibit substantially improved optical properties along with enhanced stability (Figure S2). The absorption spectra of CdSe$_x$S$_{1-x}$/CdS core/crown NPLs were presented in Figure 2b together with that of CdSe$_x$S$_{1-x}$ core NPLs for a better comparison. It is clearly seen that the excitonic features of CdSe$_x$S$_{1-x}$ core NPLs remained almost in the same spectral position with the formation of the CdS crown region, which can be explained by the unchanged quantum

confinement in the core/crown heterostructures due to the growth of the CdS region being only in the lateral direction. Furthermore, regardless of sulfur composition, a new absorption peak emerged at the same wavelength ($\sim$405 nm) in the absorption spectra of CdSe$_x$S$_{1-x}$/CdS core/crown NPLs, which corresponds to the bandgap of 4 ML thick CdS NPLs.[23] These two findings strongly support that the synthesized CdSe$_x$S$_{1-x}$ core NPLs have a homogeneously alloyed structure with the same vertical thickness. Otherwise, we would observe a shifting in the excitonic features belonging to both core and crown regions.

With the growth of CdS only in the lateral direction, CdSe$_x$S$_{1-x}$/CdS core/crown NPLs exhibit almost similar emission peaks with respect to CdSe$_x$S$_{1-x}$ core NPLs. The slightly red-shifted emission ($\sim$2−3 nm) can be related to the change in the dielectric constant.[15] Also, with the passivation of sidewalls of the CdSe$_x$S$_{1-x}$ core NPLs, CdSe$_x$S$_{1-x}$/CdS core/crown NPLs exhibit remarkable improvement in PL-QY (up to 60%) regardless of sulfur composition. For a better understanding of the increased PL-QY, we also performed time-resolved fluorescence spectroscopy (TRF) by using in-solution samples. Fluorescence decay curves of the samples were fitted by using four-exponential functions due to the complex decay kinetics observed in the NPLs.[29,30] The multiexponential decays were convolved with the instrument response function of the excitation laser to account for its pulse width ($\sim$230 ps).
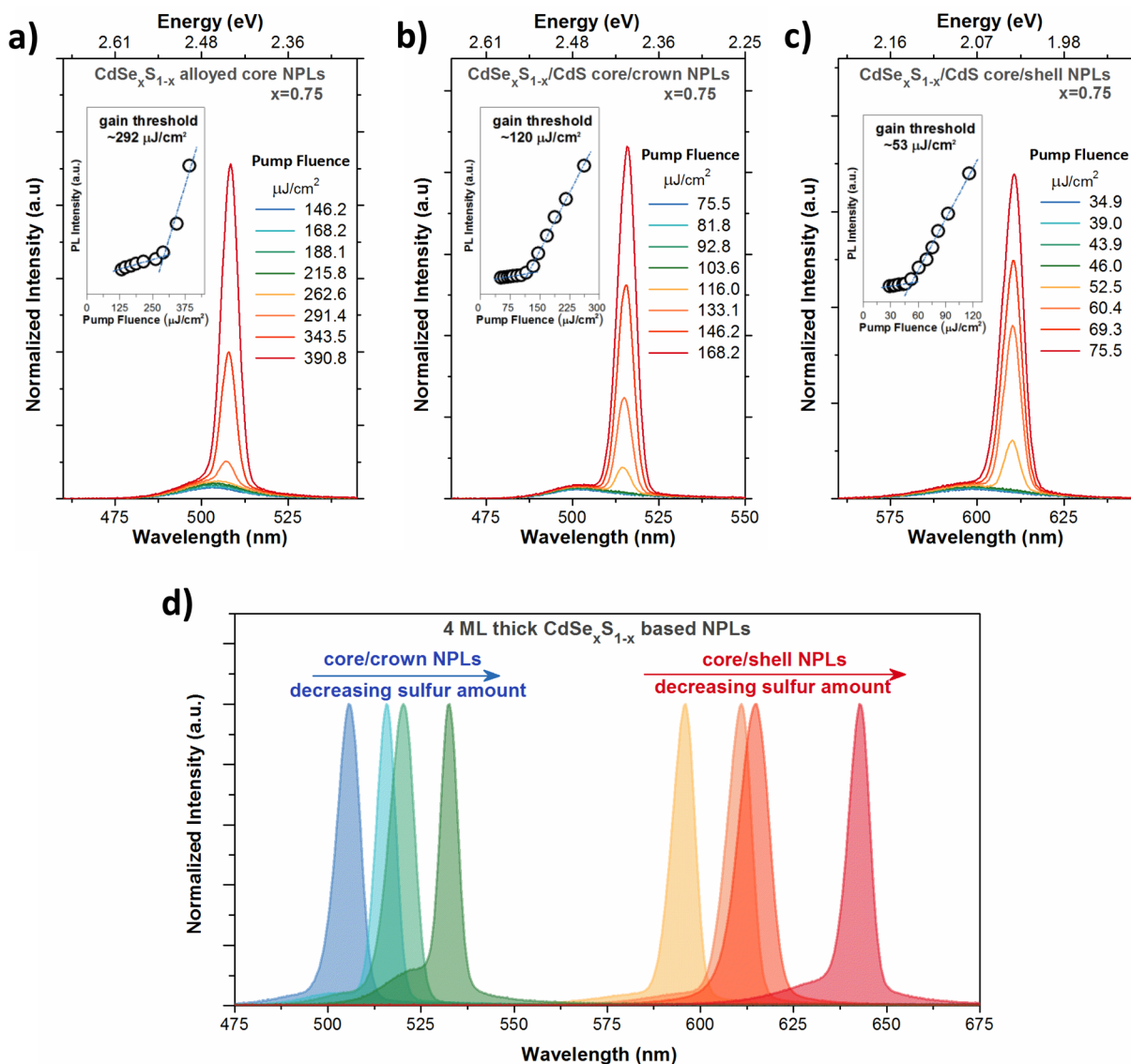
Figure 4. Optical gain performances of $CdSe_xS_{1-x}/CdS$ core/crown and core/shell NPLs having different sulfur compositions. As an exemplary case for $x = 0.75$ amplified spontaneous emission (ASE) spectra of (a) $CdSe_xS_{1-x}$ core-only NPLs, (b) $CdSe_xS_{1-x}/CdS$ core/crown NPLs, and (c) $CdSe_xS_{1-x}/CdS$ core/shell NPLs having 2 ML CdS shell at different excitation fluence. In the insets, the integrated PL intensity are given as a function of the pump fluence. (d) Normalized ASE spectra of $CdSe_xS_{1-x}/CdS$ heterostructures showing highly tunable gain performance varying with the incorporated sulfur amount.

The fluorescence decay curves and their analysis results are summarized in Figure S9 and Table S6. As an exemplary case, the decay curves of $CdSe_xS_{1-x}$ core and $CdSe_xS_{1-x}/CdS$ core/crown NPLs with $x = 0.75$ are given in Figure 2c. The amplitude-averaged fluorescence lifetime of $CdSe_xS_{1-x}$ core NPLs ($x = 0.75$) was measured to be ~0.90 ns with the fastest nonradiative decay component (0.15 ns), which is attributed to the hole trapping commonly observed in NPLs.[31,32] Thanks to the passivation of sidewalls in the $CdSe_xS_{1-x}/CdS$ core/crown NPLs, the amplitude-averaged lifetime of the core/crown NPLs ($x = 0.75$) was increased to ~3.78 ns by the suppression of the fastest nonradiative decay component.[23,24] The similar behavior was also observed for the other $CdSe_xS_{1-x}/CdS$ core/crown NPLs having different sulfur compositions, suggesting the enhanced PL-QY of the core/crown NPLs.

With the synthesis of $CdSe_xS_{1-x}/CdS$ core/crown NPLs, we obtained improved optical properties, including the enhanced

absorption cross-section and the increased PL-QY. However, due to the formation of the CdS crown region only in the lateral direction, $CdSe_xS_{1-x}/CdS$ core/crown NPLs exhibit emission almost in the same spectral position with $CdSe_xS_{1-x}$ core NPLs. In order to achieve further spectral tunability with $CdSe_xS_{1-x}$ core NPLs, we synthesized $CdSe_xS_{1-x}/CdS$ core/shell NPLs by using the colloidal atomic layer deposition (c-ALD) technique.[21] With atomically precise shell thickness control offered by the c-ALD technique, we achieved highly uniform growth of CdS layers. HAADF-STEM images of $CdSe_xS_{1-x}/CdS$ core/shell NPLs having 3 ML of CdS shell are presented in Figure 3a. As can be seen from the HAADF-STEM images, the growth of the CdS shell layer is highly uniform and $CdSe_xS_{1-x}/CdS$ core/shell NPLs preserve their initial rectangular shape during the shell growth process.

We also studied the highly tunable optical properties of $CdSe_xS_{1-x}/CdS$ core/shell NPLs. The absorption spectra of

CdSe$_x$S$_{1-x}$/CdS core/shell NPLs having different CdS shell thicknesses are presented in Figure 3b. With the formation of CdS shell layers in the vertical direction, we observed red-shifting and broadening in the excitonic features of CdSe$_x$S$_{1-x}$/CdS core/shell NPLs regardless of their sulfur compositions. While the red-shifting of excitonic features can be explained with the relaxation of the quantum confinement depending on the increased vertical thickness of NPLs, the broadening of excitonic features can be attributed to the enhanced exciton–phonon coupling.

Similarly, we observed the red-shifted emission behavior for CdSe$_x$S$_{1-x}$/CdS core/shell NPLs and achieved tunable emission within the spectral range of 560–650 nm depending on the shell thickness and sulfur composition of the starting CdSe$_x$S$_{1-x}$ core NPLs (Figure 3c). However, the PLs of CdSe$_x$S$_{1-x}$/CdS core/shell NPLs were found to be significantly broadened with respect to that of CdSe$_x$S$_{1-x}$ core NPLs. For example, CdSe core NPLs exhibit the fwhm values of ∼35−40 meV, whereas CdSe/CdS core/shell NPLs having 3 ML CdS shell have the fwhm values of 65−70 meV. In addition, we observed that the broadening of the emission bandwidths is strongly related to sulfur composition. We showed that the emission bandwidth of core/shell NPLs continuously broadened with increasing sulfur composition and reached ∼100 meV for CdSexS1−x/CdS core/shell NPLs having 3 ML CdS shell and the highest amount of sulfur composition ($x = 0.70$). This finding also supports that the broadening comes from the increased exciton–phonon coupling. Furthermore, by using in-solution samples, the formation core/shell structure was further verified with the TRF measurements. Owing to the partial separation of electron and hole wave functions in CdSe$_x$S$_{1-x}$/CdS core/shell NPLs, increased radiative fluorescence lifetimes were measured with respect to their CdSe$_x$S$_{1-x}$ cores (Figure S10). As can be seen from Figure 3d, the amplitude-averaged fluorescence lifetime was increased from ∼0.71 to ∼2.75 ns for CdSe$_x$S$_{1-x}$/CdS core/shell NPLs with $x = 0.75$ having 3 ML CdS shell. It is also important to note that when we compared the fluorescence lifetimes of CdSe$_x$S$_{1-x}$/CdS core/shell NPLs with those of CdSe$_x$S$_{1-x}$/CdS core/crown NPLs, core/shell NPLs exhibit faster fluorescence lifetimes despite their increased electron and hole wave functions delocalization. This can be attributed to the lower PL-QY of core/shell NPLs, increasing the contribution of the faster nonradiative decay components. Therefore, owing to the competition between the faster nonradiative component originating from the trap sites and the elongated radiative component with the increased electron delocalization, we observed faster fluorescence lifetimes from core/shell NPLs with respect to core/crown NPLs.

After the optical and structural characterization of CdSe$_x$S$_{1-x}$ alloyed core NPLs and their different heterostructures, we have studied their optical gain performance. For the optical gain measurements, we prepared highly close-packed films by spin coating highly concentrated NPL solutions on fused silica substrates. The samples were excited with the stripe configuration by using femtosecond laser beam (400 nm, 120 fs laser pulses at a 1 kHz repetition rate). Pump-fluence-dependent PL spectra of NPLs were collected via a fiber coupled to the spectrometer. As an exemplary case, pump-fluence-dependent PL spectra of CdSe$_x$S$_{1-x}$ core, CdSe$_x$S$_{1-x}$/CdS core/crown and core/shell NPLs ($x = 0.75$) are presented in Figure 4 (panels a−c, respectively). For the CdSe$_x$S$_{1-x}$ core only NPLs ($x = 0.75$), when the excitation fluence exceeded ∼292 μJ/cm^2, we observed slightly red-shifted (∼6 nm)

amplified spontaneous emission (ASE) peak at 508 nm having a narrower bandwidth (6−7 nm) with respect to spontaneous emission (Figure 4a). This red-shifted ASE peak can be attributed to the biexcitonic gain observed in semiconductor nanocrystals having Type-I electronic structure.[33,34] Also, while we observed comparable gain threshold for CdSe$_x$S$_{1-x}$ core NLPs having different sulfur compositions, we achieved the lowest gain threshold (∼146 μJ/cm^2) from the CdSe$_x$S$_{1-x}$ core NLPs with $x = 0.85$. Although we expected increased gain threshold from the CdSe$_x$S$_{1-x}$ core NLPs with increasing sulfur compositions owing to their decreased PL-QY and reduced absorption cross-section, CdSe$_x$S$_{1-x}$ core NLPs exhibit the relatively lower gain thresholds when compared to CdSe core NPLs. The better optical gain performance of CdSe$_x$S$_{1-x}$ core NLPs can be explained with the reduced amount of reabsorption, which seems to be a major concern of NPLs due to their almost zero Stokes-shifted emission. In addition to that, further studies including ultrafast spectroscopy should be undertaken for a better understanding of the relation between the optical gain performance and sulfur composition.

We have also studied the optical gain performance of different heterostructures of CdSe$_x$S$_{1-x}$ based NPLs. Further decreased gain thresholds are expected from CdSe$_x$S$_{1-x}$/CdS core/crown NPLs thanks to their enhanced absorption cross-section and sidewall passivation of core NPLs with the CdS crown region. As can be seen from Figure 4b, CdSe$_x$S$_{1-x}$/CdS core/crown NPLs ($x = 0.75$) exhibit a slightly red-shifted ASE peak (515 nm) with reduced gain threshold of ∼120 μJ/cm^2 in comparison to CdSe$_x$S$_{1-x}$ core only NPLs ($x = 0.75$). We also observed decreased gain threshold with the CdSe$_x$S$_{1-x}$/CdS core/crown NPLs comprising different sulfur compositions, indicating the importance of the crown formation. In addition, to further realize the spectral tunability of ASE with reduced gain threshold, we studied the optical gain performances of CdSe$_x$S$_{1-x}$/CdS core/shell NPLs having 2 ML of CdS shell. Similarly, with the formation of the CdS shell, we obtained lower gain thresholds with respect to CdSe$_x$S$_{1-x}$ core only NPLs for all sulfur compositions. From CdSe$_x$S$_{1-x}$/CdS core/shell NPLs ($x = 0.75$), we achieved a red-shifted ASE peak located at ∼610 nm with the lowest gain threshold of 53 μJ/cm^2 when compared to core-only, core/crown, and core/shell NPLs used in this study. The improved performance of core/shell NPLs can be explained with the further suppressed Auger recombination owing to partial separation of electron and hole wave functions. Also, reduced amount of reabsorption enable us to achieve decreased gain thresholds with CdSe$_x$S$_{1-x}$ based heterostructures of NPLs despite their lower PL-QY.

Finally, as it can be seen from Figure 4d, with the synthesis of alloyed heterostructures of CdSe$_x$S$_{1-x}$ core NPLs, we have achieved extended spectral tunability of the optical gain obtained from colloidal NPLs. In previous studies, low-threshold optical gain has been demonstrated by using colloidal NPLs emitting in the blue, green, yellow, and red spectral regions.[7] However, thanks to pure vertical quantum confinement, they exhibit discrete ASE peaks at ∼490 nm for blue-, ∼534 nm for green-, 575 nm for yellow-, and ∼640 nm for red-emitting NPLs. Here, by using CdSe$_x$S$_{1-x}$/CdS core/crown and core/shell NPLs, we have accomplished filling in the gaps and shown tunable ASE peaks within the range of 500−535 nm and 590−640 nm. Here it is also possible to further extend the spectral tunability by tailoring the sulfur composition of CdSe$_x$S$_{1-x}$ core-only NPLs and adjusting the thickness of the CdS shell.

In conclusion, we have reported the synthesis of core/crown and core/shell heterostructures of $CdSe_xS_{1-x}$ core-only NPLs together with their resulting excitonic properties, enabling the achievement of highly tunable and low-threshold gain performance. With the synthesis $CdSe_xS_{1-x}$/CdS core/crown NPLs, we demonstrated improved PL-QY, enhanced absorption cross-section, and increased stability without changing the emission spectra of $CdSe_xS_{1-x}$ core-only NPLs. On the other hand, with the synthesis of $CdSe_xS_{1-x}$/CdS core/shell NPLs, we realized highly tunable emission for NPLs covering a wide range of the spectrum between 560 and 650 nm, depending on the sulfur composition and shell thickness. Also, we studied the optical gain performances of different heterostructures of $CdSe_xS_{1-x}$ alloyed NPLs, offering great advantages including reduced reabsorption and spectrally tunable optical gain range. Considering the emission of $CdSe_xS_{1-x}$ based NPLs covering a wide spectral range, we demonstrated highly tunable ASE with low gain thresholds ($\sim$53 μJ/cm^2). These findings have shown the importance of the colloidal synthesis of engineered heterostructured NPLs for the achievement of superior excitonic properties and the significant potential for the utilization of NPLs for the next-generation optoelectronic devices including lasers and light-emitting-diodes (LEDs), owing to their profoundly tunable excitonic properties.

■ ASSOCIATED CONTENT

ⓈSupporting Information

The Supporting Information is available free of charge on the ACS Publications website at DOI: 10.1021/acs.chemmater.7b00829.

Photoluminescence quantum yield (PL-QY) of different heterostructures of $CdSe_xS_{1-x}$ NPLs, photoluminescence excitation spectra (PLE) of $CdSe_xS_{1-x}$ NPLs, HAADF-STEM images of $CdSe_xS_{1-x}$ NPLs showing their vertical thicknesses, analysis of high-resolution XPS spectra of $CdSe_xS_{1-x}$ NPLs, EDX spectra of $CdSe_xS_{1-x}$ NPLs, absorption and photoluminescence spectra of different heterostructures of $CdSe_xS_{1-x}$ NPLs, time-resolved fluorescence decay curves of different heterostructures of $CdSe_xS_{1-x}$ NPLs together with their analysis, amplified spontaneous emission (ASE) spectra of different heterostructures of $CdSe_xS_{1-x}$ NPLs (PDF)

■ AUTHOR INFORMATION

Corresponding Author
*E-mail: volkan@bilkent.edu.tr and hvdemir@ntu.edu.sg.

ORCID ⓘ
Hilmi Volkan Demir: 0000-0003-1793-112X

Author Contributions
§Y.K. and D.D. contributed equally to this work.

Notes
The authors declare no competing financial interest.

■ ACKNOWLEDGMENTS

■ REFERENCES

(1) Lhuillier, E.; Pedetti, S.; Ithurria, S.; Nadal, B.; Heuclin, H.; Dubertret, B. Two-Dimensional Colloidal Metal Chalcogenides Semiconductors: Synthesis, Spectroscopy, and Applications. *Acc. Chem. Res.* **2015**, *48* (1), 22−30.

(2) Nasilowski, M.; Mahler, B.; Lhuillier, E.; Ithurria, S.; Dubertret, B. Two-Dimensional Colloidal Nanocrystals. *Chem. Rev.* **2016**, *116* (18), 10934−10982.

(3) Ithurria, S.; Dubertret, B. Quasi 2D Colloidal CdSe Platelets with Thicknesses Controlled at the Atomic Level. *J. Am. Chem. Soc.* **2008**, *130* (49), 16504−16505.

(4) Ithurria, S.; Tessier, M. D.; Mahler, B.; Lobo, R. P. S. M.; Dubertret, B.; Efros, A. L. Colloidal Nanoplatelets with Two-Dimensional Electronic Structure. *Nat. Mater.* **2011**, *10* (12), 936−941.

(5) Yeltik, A.; Delikanli, S.; Olutas, M.; Kelestemur, Y.; Guzelturk, B.; Demir, H. V. Experimental Determination of the Absorption Cross-Section and Molar Extinction Coefficient of Colloidal CdSe Nanoplatelets. *J. Phys. Chem. C* **2015**, *119* (47), 26768−26775.

(6) Kunneman, L. T.; Tessier, M. D.; Heuclin, H.; Dubertret, B.; Aulin, Y. V.; Grozema, F. C.; Schins, J. M.; Siebbeles, L. D. a. Bimolecular Auger Recombination of Electron−Hole Pairs in Two-Dimensional CdSe and CdSe/CdZnS Core/Shell Nanoplatelets. *J. Phys. Chem. Lett.* **2013**, *4* (21), 3574−3578.

(7) She, C.; Fedin, I.; Dolzhnikov, D. S.; Dahlberg, P. D.; Engel, G. S.; Schaller, R. D.; Talapin, D. V. Red, Yellow, Green, and Blue Amplified Spontaneous Emission and Lasing Using Colloidal CdSe Nanoplatelets. *ACS Nano* **2015**, *9* (10), 9475−9485.

(8) Grim, J. Q.; Christodoulou, S.; Di Stasio, F.; Krahne, R.; Cingolani, R.; Manna, L.; Moreels, I. Continuous-Wave Biexciton Lasing at Room Temperature Using Solution-Processed Quantum Wells. *Nat. Nanotechnol.* **2014**, *9* (11), 891−895.

(9) She, C.; Fedin, I.; Dolzhnikov, D. S.; Demortière, A.; Schaller, R. D.; Pelton, M.; Talapin, D. V. Low-Threshold Stimulated Emission Using Colloidal Quantum Wells. *Nano Lett.* **2014**, *14* (5), 2772−2777.

(10) Kelestemur, Y.; Guzelturk, B.; Erdem, O.; Olutas, M.; Gungor, K.; Demir, H. V. Platelet-in-Box Colloidal Quantum Wells: CdSe/CdS@CdS Core/Crown@Shell Heteronanoplatelets. *Adv. Funct. Mater.* **2016**, *26* (21), 3570−3579.

(11) Guzelturk, B.; Kelestemur, Y.; Olutas, M.; Delikanli, S.; Demir, H. V. Amplified Spontaneous Emission and Lasing in Colloidal Nanoplatelets. *ACS Nano* **2014**, *8* (7), 6599−6605.

(12) Diroll, B. T.; Talapin, D. V.; Schaller, R. D. Violet-to-Blue Gain and Lasing from Colloidal CdS Nanoplatelets: Low-Threshold Stimulated Emission Despite Low Photoluminescence Quantum Yield. *ACS Photonics* **2017**, *4* (3), 576−583.

(13) Li, M.; Zhi, M.; Zhu, H.; Wu, W.-Y.; Xu, Q.-H.; Jhon, M. H.; Chan, Y. Ultralow-Threshold Multiphoton-Pumped Lasing from Colloidal Nanoplatelets in Solution. *Nat. Commun.* **2015**, *6*, 8513.

(14) Ithurria, S.; Bousquet, G.; Dubertret, B. Continuous Transition from 3D to 1D Confinement Observed during the Formation of CdSe Nanoplatelets. *J. Am. Chem. Soc.* **2011**, *133* (9), 3070−3077.

(15) Tessier, M. D.; Spinicelli, P.; Dupont, D.; Patriarche, G.; Ithurria, S.; Dubertret, B. Efficient Exciton Concentrators Built from Colloidal Core/Crown CdSe/CdS Semiconductor Nanoplatelets. *Nano Lett.* **2014**, *14* (1), 207−213.

(16) Prudnikau, A.; Chuvilin, A.; Artemyev, M. CdSe−CdS Nanoheteroplatelets with Efficient Photoexcitation of Central CdSe Region through Epitaxially Grown CdS Wings. *J. Am. Chem. Soc.* **2013**, *135* (39), 14476−14479.

(17) Delikanli, S.; Guzelturk, B.; Hernández-Martínez, P. L.; Erdem, T.; Kelestemur, Y.; Olutas, M.; Akgul, M. Z.; Demir, H. V. Continuously Tunable Emission in Inverted Type-I CdS/CdSe

Core/Crown Semiconductor Nanoplatelets. *Adv. Funct. Mater.* **2015**, 25 (27), 4282−4289.

(18) Pedetti, S.; Ithurria, S.; Heuclin, H.; Patriarche, G.; Dubertret, B. Type-II CdSe/CdTe Core/Crown Semiconductor Nanoplatelets. *J. Am. Chem. Soc.* **2014**, 136 (46), 16430−16438.

(19) Kelestemur, Y.; Olutas, M.; Delikanli, S.; Guzelturk, B.; Akgul, M. Z.; Demir, H. V. Type-II Colloidal Quantum Wells: CdSe/CdTe Core/Crown Heteronanoplatelets. *J. Phys. Chem. C* **2015**, 119 (4), 2177−2185.

(20) Mahler, B.; Nadal, B.; Bouet, C.; Patriarche, G.; Dubertret, B. Core/Shell Colloidal Semiconductor Nanoplatelets. *J. Am. Chem. Soc.* **2012**, 134 (45), 18591−18598.

(21) Ithurria, S.; Talapin, D. V. Colloidal Atomic Layer Deposition (c-ALD) Using Self-Limiting Reactions at Nanocrystal Surface Coupled to Phase Transfer between Polar and Nonpolar Media. *J. Am. Chem. Soc.* **2012**, 134 (45), 18585−18590.

(22) Pedetti, S.; Nadal, B.; Lhuillier, E.; Mahler, B.; Bouet, C.; Abécassis, B.; Xu, X.; Dubertret, B. Optimized Synthesis of CdTe Nanoplatelets and Photoresponse of CdTe Nanoplatelets Films. *Chem. Mater.* **2013**, 25 (12), 2455−2462.

(23) Li, Z.; Qin, H.; Guzun, D.; Benamara, M.; Salamo, G.; Peng, X. Uniform Thickness and Colloidal-Stable CdS Quantum Disks with Tunable Thickness: Synthesis and Properties. *Nano Res.* **2012**, 5 (5), 337−351.

(24) Maiti, P. S.; Houben, L.; Bar-Sadan, M. Growth Schemes of Tunable Ultrathin CdS X Se 1− X Alloyed Nanostructures at Low Temperatures. *J. Phys. Chem. C* **2015**, 119 (19), 10734−10739.

(25) Maiti, P. S.; Bar Sadan, M. Tuning the Surface Properties of Alloyed CdS X Se 1−x 2D Nanosheets. *RSC Adv.* **2015**, 5 (122), 100834−100837.

(26) Fan, F.; Kanjanaboos, P.; Saravanapavanantham, M.; Beauregard, E.; Ingram, G.; Yassitepe, E.; Adachi, M. M.; Voznyy, O.; Johnston, A. K.; Walters, G.; Kim, G.-H.; Lu, Z.-H.; Sargent, E. H. Colloidal CdSe 1− X S X Nanoplatelets with Narrow and Continuously-Tunable Electroluminescence. *Nano Lett.* **2015**, 15 (7), 4611−4615.

(27) de Mello, J. C.; Wittmann, H. F.; Friend, R. H. An Improved Experimental Determination of External Photoluminescence Quantum Efficiency. *Adv. Mater.* **1997**, 9 (3), 230−232.

(28) Tessier, M. D.; Mahler, B.; Nadal, B.; Heuclin, H.; Pedetti, S.; Dubertret, B. Spectroscopy of Colloidal Semiconductor Core/Shell Nanoplatelets with High Quantum Yield. *Nano Lett.* **2013**, 13 (7), 3321−3328.

(29) Rabouw, F. T.; van der Bok, J. C.; Spinicelli, P.; Mahler, B.; Nasilowski, M.; Pedetti, S.; Dubertret, B.; Vanmaekelbergh, D. Temporary Charge Carrier Separation Dominates the Photoluminescence Decay Dynamics of Colloidal CdSe Nanoplatelets. *Nano Lett.* **2016**, 16 (3), 2047−2053.

(30) Tessier, M. D.; Javaux, C.; Maksimovic, I.; Loriette, V.; Dubertret, B. Spectroscopy of Single CdSe Nanoplatelets. *ACS Nano* **2012**, 6 (8), 6751−6758.

(31) Kunneman, L. T.; Schins, J. M.; Pedetti, S.; Heuclin, H.; Grozema, F. C.; Houtepen, A. J.; Dubertret, B.; Siebbeles, L. D. A. Nature and Decay Pathways of Photoexcited States in CdSe and CdSe/CdS Nanoplatelets. *Nano Lett.* **2014**, 14 (12), 7039−7045.

(32) Guzelturk, B.; Erdem, O.; Olutas, M.; Kelestemur, Y.; Demir, H. V. Stacking in Colloidal Nanoplatelets: Tuning Excitonic Properties. *ACS Nano* **2014**, 8 (12), 12524−12533.

(33) Cihan, A. F.; Kelestemur, Y.; Guzelturk, B.; Yerli, O.; Kurum, U.; Yaglioglu, H. G.; Elmali, A.; Demir, H. V. Attractive versus Repulsive Excitonic Interactions of Colloidal Quantum Dots Control Blue- to Red-Shifting (and Non-Shifting) Amplified Spontaneous Emission. *J. Phys. Chem. Lett.* **2013**, 4 (23), 4146−4152.

(34) Kelestemur, Y.; Cihan, A. F.; Guzelturk, B.; Demir, H. V. Type-Tunable Amplified Spontaneous Emission from Core-Seeded CdSe/CdS Nanorods Controlled by Exciton−exciton Interaction. *Nanoscale* **2014**, 6 (15), 8509.